LAWRENCE
LIVERMORE
NATIONAL
LABORATORY

UCRL-JRNL-226331

Revisiting the Cape Cod Bacteria Injection Experiment Using a Stochastic Modeling Approach

R. M. Maxwell, C. Welty, R. W. Harvey

November 27, 2006

Environmental Science and Technology

Disclaimer

Revisiting the Cape Cod Bacteria Injection Experiment Using a Stochastic Modeling Approach

Reed M. Maxwell
Atmospheric, Earth, and Energy Sciences Department
Lawrence Livermore National Laboratory (L-208)
7000 East Avenue
Livermore, California 94550
maxwell5@llnl.gov

Claire Welty
University of Maryland, Baltimore County (UMBC)
Department of Civil and Environmental Engineering and
Center for Urban Environmental Research and Education
1000 Hilltop Circle, TRC 102
Baltimore, MD 21250
weltyc@umbc.edu

Ronald W. Harvey
U.S. Geological Survey
3215 Marine St., Ste. E-127
Boulder, CO 80303
rwharvey@usgs.gov.

November 7, 2006

To be submitted to

Environmental Science and Technology
UCRL-JRNL-226331

Abstract

Bromide and resting-cell bacteria tracer tests carried out in a sand and gravel aquifer at the USGS Cape Cod site in 1987 were reinterpreted using a three-dimensional stochastic approach and Lagrangian particle tracking numerical methods. Bacteria transport was strongly coupled to colloid filtration through functional dependence of local-scale colloid transport parameters on hydraulic conductivity and seepage velocity in a stochastic advection-dispersion/attachment-detachment model. Information on geostatistical characterization of the hydraulic conductivity (K) field from a nearby plot was utilized as input that was unavailable when the original analysis was carried out. A finite difference model for groundwater flow and a particle-tracking model of conservative solute transport was calibrated to the bromide-tracer breakthrough data using the aforementioned geostatistical parameters. An optimization routine was utilized to adjust the mean and variance of the lnK field over 100 realizations such that a best fit of a simulated, average bromide breakthrough curve is achieved. Once the optimal bromide fit was accomplished (based on adjusting the lnK statistical parameters in unconditional simulations), a stochastic particle-tracking model for the bacteria was run without adjustments to the local-scale colloid transport parameters. Good predictions of the mean bacteria breakthrough data were achieved using several approaches for modeling components of the system. Simulations incorporating the recent Tufenkji and Elimelech [1] equation for estimating single collector efficiency were compared to those using the Rajagopalan and Tien [2] model. Both appeared to work equally well at predicting mean bacteria breakthrough using a constant mean bacteria diameter for this set of field conditions, with the Rajagopalan and Tien model yielding approximately a 30% lower

peak concentration and less tailing than the Tufenkji and Elimelech formulation. Simulations using a distribution of bacterial cell diameters available from original field notes yielded a slight improvement in the model and data agreement compared to simulations using an average bacteria diameter; variable bacterial cell diameters lowered the modeled peak concentrations and more significantly diminished the tailing behavior, particularly for the Rajagopalan and Tien model of collision frequency. Spatial variability in detachment had little effect on the results. The Lagrangian particle transport model representing the non-idealities of the colloid transport process appears to be a robust, grid-free method for modeling field-scale distribution problems where incorporation of fine-scale heterogeneity would necessitate large numbers of computational cells. The stochastic approach based on estimates of local-scale parameters for the bacteria-transport process both captures the mean field behavior of bacteria transport and calculates an envelope of uncertainty that brackets the observations in most simulation cases.

1. Introduction

As waterborne disease outbreaks continue to be reported [3] and detailed field surveys reveal the presence of pathogens in groundwater (e.g.,[4-10]), it is clear that there is a continuing need to advance our ability to predict the transport of pathogens from their sources to drinking water supplies. Such quantification is necessary for carrying out risk assessment of waterborne pathogen transmission to humans, and in development of pathogen TMDLs [11]. Implementation of mechanistic mathematical models is one approach that can be used, but application is complicated by site-specific geologic heterogeneity and uncertainties relating to parameterizing non-ideal transport properties of bacteria and viruses in aquifer materials. Over the past 25 years, controlled laboratory studies involving homogeneous media have resulted in considerable progress towards quantifying the roles of microbial (size, shape, surface chemistry), mineral, and fluid properties on the transport of microorganisms through the terrestrial subsurface (see reviews by [12, 13]). Gains have also been made in the area of field-scale modeling by coupling porous-media transport models with a realistic representation of the microbial attachment process (e.g. [14, 15]). Less progress has been made in coupling the known non-idealities of microbial transport with a realistic representation of aquifer heterogeneity to quantify the effects of heterogeneity on the transport process (e.g. [16-19]). However, the latter type of work is needed to produce models that better capture the field-scale reality of this complex process.

Since earlier attempts to couple colloid filtration with the advection-dispersion equation to model the movement of indigenous, uncultured bacteria in a controlled field-scale tracer tests (e.g. [14]), considerable advances have been made in (1) quantifying,

statistically, aquifer heterogeneity; (2) capturing heterogeneity using numerical methods incorporating finely-gridded systems and grid-free transport algorithms; (3) refining the relationship between colloid filtration (sorptive removal) and physical heterogeneity, and (4) parameterizing the colloid filtration process. The purpose of this paper is to utilize improvements in these four areas to revisit the data interpretation from the 1991 paper by Harvey and Garabedian. We make use of the geostatistical characterization of the hydraulic conductivity heterogeneity that has been carried out for the Cape Cod site, ; particle-tracking numerical techniques that allow us to model the tracer test on a very fine grid and also allow for consideration of a distribution of bacteria cell size inputs, and postulated correlations between colloid filtration and lnK as proposed by Rehmann et al. [16]. We also utilize recent improvements in estimations of the collector efficiency parameter in colloid filtration by Tufenkji and Elimelech [1], as compared to the Rajagopalan and Tien [2] model that is still widely used. This paper evaluates how these improvements affect data interpretation and highlights areas where further work is needed.

2. Methods

2.1 Field Experiment

In October 1987, a short-scale (6.8 m) natural-gradient injection test involving indigenous bacteria fluorescently labeled with the fluorochrome 4,6-diamidino-2-phenylindole (DAPI) was conducted in the sand and gravel aquifer at the U.S. Geological Survey Toxic Substances Hydrology research site at Cape Cod, Massachusetts. Details of the conditions of the injection test are provided in Harvey and Garabedian [14]; information on the site hydrogeology is provided in LeBlanc et al.[20]. In brief, a 90-L

volume of bromide solution (150 mg/L) and stained bacteria was injected at a rate of 0.85 L/m simultaneously at depths of 8.5 and 9.1 m below land surface in the saturated zone; breakthrough was measured at these elevations 6.8 m downgradient from point of injection. At about the same time the tracer test was being conducted, an extensive characterization of the nature and distribution of the hydraulic conductivity properties of aquifer sediments was being carried out at a nearby plot by means of borehole flow meter measurements [21]. The location of the two tests relative to one another is shown in plan view Figure 1. The vertical position of the injection points relative to the vertical depth over which the aquifer geostatistical information was obtained is shown in Figure 2.

Two additional data sets that were recorded during the tracer test, but not previously reported, were (1) breakthrough observations at two elevations at multilevel sampler M7, 5 m downgradient and about 1 m east of the centerline between the injection point and observation well M1, and (2) the histogram of the distribution of the sizes of the injected bacteria (Figure 3) [22].

2.2 Governing equations

The governing equation for local-scale advection, dispersion, and reversible interactions with grain surfaces for resting-cell bacteria in porous media is given by

$$\frac{\partial C_j}{\partial t} + \nabla \bullet \left(\mathbf{v} C_j\right) - \nabla \bullet \left(\mathbf{D} \bullet \nabla C_j\right) = -k_j^{att} C_j + k_j^{\det} \frac{\rho_b}{\rho n} S_j \qquad (1)$$

For attached bacteria, the mass balance equation is given by

$$\frac{\rho_b}{\rho n} \frac{\partial S_j}{\partial t} = k_j^{att} C_j - k_j^{\det} \frac{\rho_b}{\rho n} S_j \qquad (2)$$

where C_j is the mass fraction [dimensionless] of bacteria in solution of species or attribute j, S_j is the mass fraction [dimensionless] of attached bacteria of attribute j, k_j^{att}

and k_j^{det} are first-order rate constants for physical/chemical attachment (sorption) and detachment of species j, ρ and ρ_b are densities of the fluid and bulk porous medium [M/L^3], **D** is the hydrodynamic dispersion tensor [L^2/T], **v** is the average seepage velocity [L/t], and n is effective porosity [dimensionless]. Growth and death terms are not included in (1) and (2) because growth of the DAPI-stained bacteria was not observed during the test and, in a control suspension and in tracer test samples during a 30-day period following collection, growth and death were not significant [14]. Although significant advances have been made in understanding the effect of bacterial chemotaxis at the pore scale [23], much about the macroscale significance of chemotaxis for bacteria is still poorly understood [24]. However, DAPI, which is known to hamper bacterial activity [25], has recently been shown to inhibit chemotactic activity in groundwater bacteria [26]. Also, the uncultured bacteria were stored in nutrient-depleted water prior to injection in order to lessen the formation of temporal gradients in dissolved organic carbon. Consequently, the effects of chemotaxis are assumed to be minor and, therefore are not included in equations (1) and (2).

Parameterization of k_j^{att} for subsurface microbial transport in aquifers using a colloid filtration theory developed for ideal porous media was first proposed by Harvey and Garabedian [14] and has been utilized by a number of other researchers (e.g., Rehmann et al.,[16]; Schijven et al. [15]). This model is popular because it is based on fundamental thermodynamic principles, and most of its parameters are published constants or can be measured. A widely-used model for colloid filtration is that of Rajagopalan and Tien (R&T) [2], as modified by Martin et al. [27] and clarified by Logan et al. [28], which is given as:

$$k_j^{att} = \left[\frac{3}{2}\frac{(1-n)}{d_{10}}\alpha_c \eta\right] v \tag{3}$$

where v is the groundwater velocity magnitude [L/T], η is the collision frequency, or single collector efficiency [dimensionless], α_c is the collision efficiency factor, or probability that collision will result in attachment [dimensionless] and d_{10} is the sieve size [m] for which 90% of grains of the porous medium are retained. The d_{10} is used as the representative grain diameter in heterogeneous media based on the work of Martin et al. [27].

R&T estimated the collision frequency to be composed of additive factors influenced by Brownian motion, interception of the colloids by grains, and gravitational settling:

$$\eta = 4A_s^{1/3}N_{Pe}^{-2/3} + A_s N_{Lo}^{1/8} N_R^{15/8} + 0.00338 A_s N_G^{1.2} N_R^{-0.4} \tag{4}$$

where

$$A_S = \frac{2\left[1-(1-n)^{5/3}\right]}{\left[2-3(1-n)^{1/3}+3(1-n)^{5/3}-2(1-n)^2\right]}$$

$$N_R = \frac{d_p}{d_{10}}$$

$$D_p = \frac{B_z T}{3\pi\mu d_p}$$

$$N_{Pe} = \frac{nvd}{D_p} = \frac{3\pi\mu}{B_z T} nvd_{10}d_p$$

$$N_{vdW} = \frac{H}{B_z T}$$

$$N_G = \frac{2}{9}\frac{d_p^2(\rho_p - \rho)g}{4\mu v n} = \frac{d_p^2(\rho_p - \rho)g}{18\mu v n}$$

$$N_A = \frac{N_{vdW}}{N_R N_{Pe}} = \frac{4H}{12\pi\mu d_p^2 v n} = \frac{H}{3\pi\mu d_p^2 v n}$$

and H is the Hamaker constant [M/L^{2}T^2], B_z is the Boltzmann constant [M/L^{2}T$^{2\circ}$K], T is temperature (˚K), μ is dynamic viscosity [M/LT], d_p is colloid diameter [L], ρ is the fluid density [M/L^3] and ρ_p, the buoyant density of the colloidal particle [M/L^3]. A recent alternative formulation of collision frequency has been proposed by Tufenkji and Elimelech (T&E) [1], which the authors have shown to have an improved fit to lab data compared to the R&T model:

$$\eta = 2.4 A_s^{1/3} N_R^{-0.081} N_{Pe}^{-0.715} N_{vdW}^{0.052} + 0.55 A_s N_R^{1.675} N_A^{0.125} + 0.22 N_R^{-0.24} N_G^{1.11} N_{vdW}^{0.053} \quad (5)$$

Physical interpretations of the dimensionless parameters in Equations 4 and 5 can be found in Table 1 of Tufenkji and Elimelech [1].

2.3 Effect of Hydraulic Conductivity Variability on Microbial Transport

Hess et al. [21] have shown that the three-dimensional distribution of the natural-logarithm of hydraulic conductivity (lnK) of the aquifer material at the Cape Cod site can be represented as a stationary, correlated random field on the scale of tens of meters. Of interest is how this spatial variability in lnK couples with and affects the colloid transport process as represented by (1) and (2). It is well known that lnK affects the fluid velocity (v) directly through Darcy's law. For the colloid transport case there is additional nonlinear dependence on lnK through the expression for attachment. From (3) it can be seen that

$$k_j^{att} = f(v, lnK) \quad (6)$$

Dependence on v is direct as well as through the expression for $\eta(v)$ given by (4) or (5). k_j^{att} is also dependent on lnK in η through known correlations between d_{10} and lnK, and through postulated relationships between α_c and lnK. To obtain a d_{10}-lnK relationship, we inverted the Hazen [29] formula

$$d_{10} = [10^{-4}\exp(\ln K)]^{0.5} \tag{7}$$

where K and d_{10} are in m/sec and m, respectively. Good agreement has been shown between local-scale K calculated using the Hazen formula from grain-size analysis and K measured on the same sample using a constant-head permeameter [30], for the Cape Cod data.

Correlations of the transport parameters α_c, and $k_j^{\det}$ with lnK have been postulated by Rehmann et al. [16] to be:

$$\alpha_c = a_1 + b_1 \ln K + \delta_1 \tag{8}$$

$$k_j^{\det} = a_2 + b_2 \ln K + \delta_2 \tag{9}$$

where a_i and b_i are constants, and δ_i is the zero-mean random fields accounting for the portions of α_c and $k_j^{\det}$ not correlated with ln K [31, 32]. The general forms specified by (8) and (9) allow positive ($b_i > 0$), negative ($b_i < 0$), or zero ($b_i = 0$) correlation with the lnK field. The uncorrelated portion δ_i accounts for spatial variability in conditions not related to the hydraulic conductivity of the porous medium (e.g., solution chemistry). Numerical values for a_i, b_i, and δ_i must be determined experimentally. An example data set showing the linear correlation of α_c and lnK is given by Ren et al. [33].

In order to prevent α_c from going to zero for large values of lnK, we have found that an alternative formula for (8) specified as

$$\alpha_c = a_3 \exp(-b_3 \ln K) + \delta_3 \quad (10)$$

is computationally advantageous. Figure 4 shows both the linear fit (Eq. 8) and the exponential fit (Eq. 10) to data taken from Ren et al. [33] and Dong et al.[34] (as expanded upon in Mailloux et al. [35], Figure 10c) covering a wide range of lnK values.

2.4 Numerical Solution Using a Particle Tracking Approach

A Lagrangian, particle-tracking approach was used to simulate both bromide and bacterial transport. Particle-tracking methods have been widely applied in subsurface transport problems (e.g. [36-39]). This approach transforms transport equations (1)-(2) into a set of discrete particles that each represents a small portion of the total mass of solute. A modification to the particle-tracking approach for a conservative tracer was used to represent the attached bacterial phase and the attachment/detachment kinetics presented in Section 2.2. This modification represents attachment and detachment rates as particle probability functions. For a given particle timestep, an attachment or detachment probability is calculated and a random function is used to determine whether a given particle attaches to the soil matrix. This approach is similar to that introduced by Valocchi and Quinodoz [40] and Michalak and Kitanidis [41] for modeling kinetic chemical sorption and has been used to model matrix diffusion (e.g. Liu et al.[42]). For large problems with heterogeneous physical parameters, this approach of representing attachment-detachment interactions as particle probabilities facilitates rapid solution of Equations (1)-(2) with mass conservation and no numerical dispersion. Also, each particle is moved according to a locally calculated, optimal time step, and particles may be split into two particles of equal mass if a single particle occupies a computational cell. These techniques further improve the efficiency and accuracy of the particle transport

model, particularly to very accurately resolve low concentrations [43]. Details of this model are provided in the Supporting Information provided with this manuscript.

2.5 Generation of Hydraulic Conductivity Random Field

The two alluvial layers identified in Harvey and Garabedian [14] were conceptualized as having small-scale hydraulic conductivity (K) heterogeneity following a correlated, Gaussian random field, each with independent statistical parameters. The lnK variance (σ_{lnK}^2) and correlation scales (λ_x=λ_y, λ_z) were taken as those reported by Hess et al. [21] from a nearby plot, and information reported by Harvey and Garabedian [14] was used to estimate initial values of the geometric mean K values for the two layers (Table 1). Using these statistical parameters, the small-scale variability in hydraulic conductivity of each layer was generated numerically using the turning bands approach of Tompson et al. [44]. Because measurements made by Hess et al. [21] were not located directly in the Harvey and Garabedian [14] study plot, realizations of the hydraulic conductivity random field were not conditioned on the field data; i.e., unconditional simulations were utilized.

Adjustment of the initial hydraulic conductivity field to obtain the best fit of simulated bromide transport to that measured by Harvey and Garabedian was carried out as follows. A flow model, 17.0 x 10.2 x 3.8 m in the x, y and z dimensions, respectively, was constructed with a 0.34 m and 0.038 m lateral and vertical spatial discretization (dx=dy, dz), respectively, creating 50 x 30 x 100 finite difference cells (nx, ny and nz). The finite-difference flow code ParFlow [45-47] was run for 100 realizations of the hydraulic conductivity field. The model was simulated as steady-state flow and constructed with constant head boundaries on the X0 and Xmax faces and no-flow on all

others to provide the observed gradient listed in Table 1. A bromide tracer was introduced as a pulse source of particles in a 0.464 m x 0.56 m x 1 m volume centered on M02 (6.8 m upgradient of M01) to achieve approximately the same injection conditions as the Harvey and Garabedian [14] field experiment. This is shown in Figure 2 along with other schematic details of the simulation domain. The average of the breakthrough curves generated by forward simulation over the 100 geostatistical realizations was compared to breakthrough field data for all four locations (wells M01 and M07, two upper, two lower). The parameter estimation code, PEST [48] was used to adjust the geometric mean K and lnK variance for the two layers using the difference between calculated average (over all 100 realizations) and observed bromide concentrations for all four monitoring locations as the objective function. (The correlation scales were not adjusted.) This process was run iteratively until the objective functions converged. At this point, a best fit to the bromide data was achieved and the lnK statistical parameters used to generate the optimal set of 100 realizations of the lnK field and the resulting 100 lnK realizations and flow fields were saved and used for the bacteria simulations. Table 2 provides the numerical parameters used in the flow and transport models.

2.6 Bacteria Transport Simulations

Bacteria injection and downgradient transport was simulated using the flow fields resulting from the 100 hydraulic conductivity realizations generated by the bromide calibration. Bacteria transport was modeled using several options: (1) the R&T vs. T&E formulations for attachment; (2) average vs. particle size distribution for the bacteria sizes, and (3) constant vs. variable detachment rates. This resulted in seven different bacterial transport cases, each of which was run over all 100 realizations of hydraulic

conductivity. Although the community of unattached bacteria comprising the injectate included many rod-shaped cells, this model assumes uniform spherical morphology. In all bacterial transport runs, η was spatially variable, with grain diameter related to *ln*(K) (using the Hazen formula, Equation 7), the velocity taken to be the magnitude of the local cell velocities, and α_c related to ln(K) using Equation 10 as described in Section 2.3. This overall approach for relating filtration parameters to hydraulic conductivity is similar to that presented in Maxwell et al. [19]. Using the same initial condition as the bromide runs, the bacteria were introduced as a pulse source of particles in a 0.464 m x 0.560 m x 1.00 m volume centered on M02. For each of the aforementioned seven cases, the average of the bacteria breakthrough curves generated by simulation over the 100 geostatistical realizations was compared to the field data for all four locations (upper and lower sampled ports of wells M01 and M07,). Table 1 provides the physical input data used in the bacteria transport simulations. For all simulations, the estimated value of local dispersivity (0.0005 m) had little effect compared to mixing due to heterogeneity, and therefore all runs were carried out with this parameter set equal to zero for computational efficiency.

3. Results

The results of the bromide calibration are given in Figure 5. The model results are depicted as the arithmetic mean over 100 realizations (heavy solid line) with the mean plus one standard deviation (over 100 realizations), plotted as a thin dashed line. The mean minus one standard deviation was zero for all tracer results. Table 2 lists the

physical parameters that characterize the Gaussian random field resulting from the bromide calibration.

Plotted in Figure 6 are the observed and simulated bacterial transport concentrations at the upper and lower ports for well M01 and the lower port for well M07. (No bacteria were recovered from the upper port of M07 in the field experiment). The simulations in Figure 6 depict the attachment correlations parameterized using either the T&E expression (Figures 6 a, b, c) or the R&T equation (Figures 6 d,e,f) for a single, averaged bacteria particle size of 0.63 um. As for the bromide runs, the bacteria simulations are also plotted as the arithmetic mean (solid line) and +/- one standard deviation (dashed line) calculated over 100 realizations of the hydraulic conductivity random field. A constant detachment rate of $k_j^{det} = 0.02\ d^{-1}$ was used for all simulations.

Figure 7 shows the observed and simulated bacterial transport concentrations again use the T&E (Figure 7 a,b, c) and R&T Figures 7 d, e, f) expressions for bacterial attachment but instead of a constant bacteria diameter, the distribution of 10 bacteria diameters shown in Figure 3 was utilized. These simulations are also plotted as the arithmetic mean (solid line) and +/- one standard deviation (dashed line) calculated over 100 realizations of the hydraulic conductivity random field. Again a constant detachment rate of $k_j^{det} = 0.02\ d^{-1}$ was used for all simulations.

Figure 8 shows plots of simulations versus observations at all wells for the bromide and bacteria cases presented in Figures 5 - 7, with a linear regression through the data points and a 1:1 line (which would be a perfect fit) superimposed for comparison.

4. Discussion

The Figure 5 plots show a remarkably good agreement between observed and mean simulated peak bromide concentrations at the M01 upper and lower wells and the M07 lower well. Although simulation of peak bromide concentration at the M07 upper well is not as good as the three others – it is a factor of four higher than the observation -- the simulated breakthrough curve does capture the approximately correct width of the observed bromide breakthrough at this location, and falls within the +/- one standard deviation of the mean simulation. For all wells other than M01 lower, the mean model first appearance of bromide precedes the observed data, indicating some error in the modeled lnK field compared to the in-situ field. Nonetheless, the overall good agreement is borne out by the plot in Figure 8a – the slope of the best fit line through the observation versus simulation of all points at all wells is 0.96, with an R^2 of 0.88.

All of the simulated mean bromide concentrations fall within the envelope encompassed by +/- one model standard deviation. While this envelope may visually appear to be quite large for all wells, it should be recognized that this is due to the nature of the simulations, which were unconditional. However, if K data were available within the model domain on which the random fields could be conditioned, the standard deviation would be tighter. Given the overall good match of the simulated mean bromide to the breakthrough data, we have confidence that the heterogeneity of the test site is fairly well represented by the model results. We also point out that by using the numerical technique, where the heterogeneity is specified explicitly, we are not restricted from modeling transport over small distances, whereas this would be a problem using a small-perturbation stochastic analytical approach (e.g., Rehmann et al. [16]) that requires

transport over many correlation scales of a heterogeneous K field in order to satisfy ergodicity requirements.

Figure 6 shows the simulations of resting cell bacteria assuming a mean, constant bacteria diameter as input, for both the T&E and R&T models. All local-scale bacteria transport parameters were approximated from literature values and input to the model before running; there was no parameter fitting involved and the same 100 lnK realizations and flow fields were used from the bromide calibrations. For all wells, the simulated mean bacteria concentrations agree with the observations, and generally the observed data fall within +/- one standard deviation of the simulated mean. The simulated fist arrival times of the bacteria at the M01 upper and M07 lower wells precede the first arrival of the observed data by several days, which is to be expected given the bromide results. Both the R&T and T&E colloid transport models appear to do an equal job in the model predictions using the constant bacteria diameter. This is confirmed by the plots in Figures 8b and 8c – the slopes of the linear regressions to the simulated versus observed data are 0.86 and 1.37 for the R&T and T&E cases, respectively, compared to a perfect fit of 1.0. Both models consistently overpredict the tailing behavior compared to the observations. Observed concentrations past 25 days do not fall within +/- one standard deviation of the simulated mean for well M01 upper or lower port.

Incorporation of the distribution of bacteria diameters in the numerical model, as illustrated by Figure 7, yields a slight improvement in model and data agreement, compared to Figure 6, most noticeably in the breakthrough after 25 days. In this case, the peak simulated breakthrough values of mean bacteria concentration are lower than for the

constant-mean bacteria-diameter case and the widths of the breakthrough curves are also in better agreement. The slopes of the linear regressions in Figure 8 show about a 10% improvement for the T&E formulation (1.37 in Figure 8c compared to 1.24 in Figure 8e) while linear regression slopes do not change as much in the R&T formulation. The bacteria diameter affects the transport process in the expression for single collector efficiency (η), where the relative effects of van der Waals forces, interception, and gravity are incorporated into the local-scale expression as given by Equations 4 or 5. Figure 7 also indicates that incorporation of the new T&E model into the expression for local-scale single collector efficiency results in larger bacteria concentrations than the R&T model. The overall difference in these two models corresponds to the lower single collector efficiency (η) predicted by the T&E formulation. This is also shown by Figures 8d and 8e – the slopes of the linear regression of the simulated versus observed data are 0.79 for the R&T and 1.24 for the T&E models. Figures 2 and 3 in Tufenkji and Elimelech [1] compare the single collector efficiencies calculated for a range of particle diameters for the R&T and T&E formulations. The range of particle diameters simulated in this current study correspond to the region of largest difference between the two models.

Figures 5 and 6 show model results utilizing a constant detachment rate. The model was also run for the T&E case using a detachment rate correlated to hydraulic conductivity, thereby rendering a spatially variable detachment rate. These model runs showed that spatial variability of detachment had little effect on breakthrough compared to the constant mean detachment case, i.e., the model results appeared to be virtually identical to Figure 7 and therefore are not shown. Figure 8f shows the results of the

simulated vs. observed data for this case for all wells and it can be seen is virtually identical to Figure 8e. The value of the detachment rate affects the tailing behavior of the breakthrough curves, and this was not captured well either using a constant or spatially-variable detachment rate.

5. Summary

We have reinterpreted breakthrough data for bromide and resting-cell bacteria injection tests carried out in 1987 at the USGS Cape Cod site as reported in Harvey and Garabedian [14] using computational tools and theoretical frameworks in large part unavailable when the first analysis of the 1987 tracer test was conducted. The purpose of conducting the simulations and analysis of the data was to illustrate the applications of these advancements. This work may have implications for those intending to use the Harvey and Garabedian model in engineering applications (e.g., Mutsvangwa et al. [49]).

Our analysis differs from that reported in 1991 in the following aspects. First, we utilized a fully-three dimensional transport model of the tracer tests, to better match the field conditions of the pulse injection in a three-dimensional flow field, whereas a one dimensional analysis was previously employed. Second, we explicitly incorporated information on the physical heterogeneity of the hydraulic conductivity field as conditioned by information on observations of conservative tracer breakthrough. Use of the methods in this paper is therefore predicated upon information on the physical heterogeneity of the field site, i.e., the hydraulic conductivity distribution, being available. This can be an expensive undertaking and is still an active area of research in the field of hydrogeology (e.g., [50, 51]). Although we modeled the hydraulic conductivity field as being stationary (constant mean and variance) based on nearby field

data, stationarity of the lnK field is not required for the numerical methods such as those used here, whereas this would be a restriction on using approaches that rely on this assumption (e.g. [16]). This method is also not restricted in applications to near-field problems where it would be expected that macroscopic behavior may be non-Fickian at such scales. Also, we utilized unconditional simulations because K data were not available in the test plot on which to condition the simulations; availability of this data would have significantly reduced the standard deviation around the mean for the simulated breakthrough curves.

Third, we were successful at simulating bacteria transport using a stochastic numerical approach with no parameter fitting of the bacteria transport and filtration parameters. After calibrating 100 unconditional K random field realizations based on optimization of the mean and standard deviation of the lnK field to provide a best fit of the bromide breakthrough curves, we were able to show very good simulation of bacteria transport/filtration where the local scale parameters – collision efficiency factor and single collector efficiency – are spatially variable owing to postulated correlation with hydraulic conductivity variability. The prediction of the bacteria breakthrough was improved in the T&E formulation through incorporation of the distribution of bacteria diameters in the injectate, as opposed to utilizing a mean, constant bacterial diameter for the simulations. This attribute is simple to incorporate using the particle-tracking approach, where particles can be assigned variable properties such as diameter. Apparently, the dependence of the single collector efficiency on bacteria diameter is significant even for field applications owing to the relative importance of van der Waals forces vs. interception vs. gravity being dependent upon bacteria diameter in Equations 4

or 5.

Fourth, the stochastic framework utilized here, as postulated by Rehmann et al. [16], is dependent upon the assumption of correlation of the colloid filtration parameters (single collector efficiency and collision efficiency factor) and detachment with the spatial variability of hydraulic conductivity, and the availability of data to parameterize this correlation. However, such experimental data are scarce. This type of correlation data can be generated by fairly simple laboratory experiments (see e.g., Ren et al. [33]) and is expected to be fairly site specific. This type of information is needed in order to be able to determine the range of correlation parameters physically feasible. As demonstrated by hypothetical simulations in Maxwell et al. [19], the model is quite sensitive to values of the correlation parameters. Improvements can be made as published data become available on correlations between colloid transport parameters and lnK for the sedimentary materials from this field site.

We assumed a constant porosity value for these simulations, because in general porosity variability has a secondary effect on macrodispersion compared to hydraulic conductivity variability [52], owing to porosity typically varying by about +/-0.15 in granular media, whereas hydraulic conductivity typically varies over several orders of magnitude. The Hazen formula used in this paper relating grain size to the square root of hydraulic conductivity for parameterizing local-scale variability assumes a monotonic relation and positive correlation between these two variables. Recent geophysical work by Morin [53] at the Cape Cod site contributes significantly to the understanding of the relations between hydraulic conductivity, grain size and packing, and porosity, including documentation of a negative correlation between porosity and hydraulic conductivity at

this site. These findings could be quantitatively refined by obtaining sediment cores and sectioning them to determine the relationship among hydraulic conductivity, grain size, and porosity as a function of core length. Results could be used to parameterize a relation among the variables that may be more appropriate than the Hazen formula. An improved formulation could easily be incorporated into the model presented in this paper, and sensitivity of the transport process to a revised formulation could be explored.

Finally, we have only addressed the effect of physical heterogeneity on the microbial transport process in this paper. Chemical heterogeneity (e.g., iron oxide coatings) can also have a significant influence on the transport process (e.g., Tompson and Jackson [54]) and this effect can be incorporated into the model so that the interaction between physical and chemical heterogeneity can be assessed. Further work is underway to address this effect.

6. References

1. Tufenkji, N. and M. Elimelech, *Correlation equation for predicting single-collector efficiency in physicochemical filtration in saturated porous media.* Environmental Science & Technology, 2004. **38**(2): p. 529-536.
2. Rajagopalan, R. and C. Tien, *Trajectory Analysis of Deep-Bed Filtration with Sphere-in-Cell Porous-Media Model.* Aiche Journal, 1976. **22**(3): p. 523-533.
3. Blackburn, B., Craun, GF. Yoder,J ., Hill,V, Calderon, R L Chen,N, Lee, S H.. Levy, D A Beach, MJ, *Surveillance for Waterborne-Disease Outbreaks Associated with Drinking Water --- United States, 2001—2002, Morbidity and Mortality Weekly Report*. 2004, Centers for Disease Control and Prevention, October 22, 53(SS08). p. 23-45.
4. Banks, W.S.L., C.A. Klohe, and D. A. Battigelli, *Occurrence and distribution of enteric viruses in shallow ground water and factors affecting well vulnerability to microbiological contamination in Worcester and Wicomico Counties, MD*. 2001, U.S. Geological Survey, Water Resources Investigations Report 01-4147.
5. Lindsey, B.D., J.S. Rasberry, and T.M. Zimmerman, *Microbiological quality of water from noncommunity supply wells in carbonate and crystalline aquifers of Pennsylvania*. 2002, US Geological Survey, Water-Resources Investigations Report 01-4268.
6. Abbaszadegan, M., M. Lechevallier, and C. Gerba, *Occurrence of viruses in US groundwaters.* Journal American Water Works Association, 2003. **95**(9): p. 107-120.
7. Borchardt, M.A., et al., *Incidence of enteric viruses in groundwater from household wells in Wisconsin.* Applied and Environmental Microbiology, 2003. **69**(2): p. 1172-1180.
8. Borchardt, M.A., N.L. Haas, and R.J. Hunt, *Vulnerability of drinking-water wells in La Crosse, Wisconsin, to enteric-virus contamination from surface water contributions.* Applied and Environmental Microbiology, 2004. **70**(10): p. 5937-5946.
9. Powell, K.L., et al., *Microbial contamination of two urban sandstone aquifers in the UK.* Water Res, 2003. **37**(2): p. 339-52.
10. Francy, D.S., R. N. Bushon, J. Stoper, E. Luzano, and G.S. Fout, *Environmental factors and chemical and microbiological water-quality constituents related to the presence of enteric viruses in groundwater from small public water supplies in southeastern Michigan.* . 2004, U.S. Geological Survey, Scientific Investigations Report 2004-5219. p. 54 pp.
11. Agency, U.S.E.P., *Protocol for Developing Pathogen TMDLs.* . 2001, Office of Water (4503F), United States Environmental Protection Agency: Washington, DC. p. 132 pp.
12. Jin, Y. and M. Flury, *Fate and transport of viruses in porous media.* Advances in Agronomy, Vol 77, 2002. **77**: p. 39-+.
13. Schijven, J.F. and S.M. Hassanizadeh, *Removal of viruses by soil passage: Overview of modeling, processes, and parameters.* Critical Reviews in Environmental Science and Technology, 2000. **30**(1): p. 49-127.

14. Harvey, R.W. and S.P. Garabedian, *Use of Colloid Filtration Theory in Modeling Movement of Bacteria through a Contaminated Sandy Aquifer.* Environmental Science & Technology, 1991. **25**(1): p. 178-185.
15. Schijven, J.F., et al., *Modeling removal of bacteriophages MS2 and PRD1 by dune recharge at Castricum, Netherlands.* Water Resources Research, 1999. **35**(4): p. 1101-1111.
16. Rehmann, L.L.C., C. Welty, and R.W. Harvey, *Stochastic analysis of virus transport in aquifers.* Water Resources Research, 1999. **35**(7): p. 1987-2006.
17. Sun, N., et al., *A novel two-dimensional model for colloid transport in physically and geochemically heterogeneous porous media.* Journal of Contaminant Hydrology, 2001. **49**(3-4): p. 173-199.
18. Bhattacharjee, S., J.N. Ryan, and M. Elimelech, *Virus transport in physically and geochemically heterogeneous subsurface porous media.* Journal of Contaminant Hydrology, 2002. **57**(3-4): p. 161-187.
19. Maxwell, R.M., C. Welty, and A.F.B. Tompson, *Streamline-based simulation of virus transport resulting from long term artificial recharge in a heterogeneous aquifer.* Advances in Water Resources, 2003. **26**(10): p. 1075-1096.
20. Leblanc, D.R., et al., *Large-Scale Natural Gradient Tracer Test in Sand and Gravel, Cape-Cod, Massachusetts .1. Experimental-Design and Observed Tracer Movement.* Water Resources Research, 1991. **27**(5): p. 895-910.
21. Hess, K.M., S.H. Wolf, and M.A. Celia, *Large-Scale Natural Gradient Tracer Test in Sand and Gravel, Cape-Cod, Massachusetts .3. Hydraulic Conductivity Variability and Calculated Macrodispersivities.* Water Resources Research, 1992. **28**(8): p. 2011-2027.
22. Harvey, R.W., *Field Notes*. 1987.
23. Barton, J.W. and R.M. Ford, *Mathematical model for characterization of bacterial migration through sand cores.* Biotechnology and Bioengineering, 1997. **53**(5): p. 487-496.
24. Ford, R.M.a.R.W.H., *Role of chemotaxis in the transport of bacteria through saturated porous media.* Advances in Water Resources, 2006.
25. Parolin, C., et al., *The effect of the minor groove binding agent DAPI (4,6-diamidino-2-phenyl-indole) on DNA-directed enzymes: an attempt to explain inhibition of plasmid expression in Escherichia coli [corrected]*. FEMS Microbiol Lett, 1990. **56**(3): p. 341-6.
26. Toepfer, J.A., *The Impact of the Nucleic Acid Stain DAPI on the Motility and Chemotactic Behavior of the Soil-Dwelling Bacteria Pseudomonas putida F1*, in *Department of Chemical Engineering*. 2006, University of Virginia.
27. Martin, M.J., et al., *Scaling bacterial filtration rates in different sized porous media.* Journal of Environmental Engineering-Asce, 1996. **122**(5): p. 407-415.
28. Logan, B.E., et al., *Clarification of Clean-Bed Filtration Models.* Journal of Environmental Engineering-Asce, 1995. **121**(12): p. 869-873.
29. Hazen, A., *A discussion of "Dams on sand foundations" by A. C. Koenig.* Trans. Am. Soc. Civ. Eng., 1911. **73**.
30. Wolf, S.H., M.A. Celia, and K.M. Hess, *Evaluation of Hydraulic Conductivities Calculated from Multiport-Permeameter Measurements.* Ground Water, 1991. **29**(4): p. 516-525.

31. Garabedian, S.P., L. W. Gelhar, and M.A. Celia, *Large-scale dispersive transport in aquifers: Field experiments and reactive transport theory.* . 1988, MIT Parsons Lab Report 315.
32. MirallesWilhelm, F. and L.W. Gelhar, *Stochastic analysis of sorption macrokinetics in heterogeneous aquifers.* Water Resources Research, 1996. **32**(6): p. 1541-1549.
33. Ren, J.H., A.I. Packman, and C. Welty, *Correlation of colloid collision efficiency with hydraulic conductivity of silica sands.* Water Resources Research, 2000. **36**(9): p. 2493-2500.
34. Dong, H.L., et al., *Relative dominance of physical versus chemical effects on the transport of adhesion-deficient bacteria in intact cores from South Oyster, Virginia.* Environmental Science & Technology, 2002. **36**(5): p. 891-900.
35. Mailloux, B.J., et al., *The role of physical, chemical, and microbial heterogeneity on the field-scale transport and attachment of bacteria.* Water Resources Research, 2003. **39**(6): p. -.
36. Maxwell, R.M. and W.E. Kastenberg, *Stochastic environmental risk analysis: an integrated methodology for predicting cancer risk from contaminated groundwater.* Stochastic Environmental Research and Risk Assessment, 1999. **13**(1-2): p. 27-47.
37. Kinzelbach, W., *The random walk method in pollutant transport simulation*, in *Groundwater Flow and Quality Modeling*, A.G. E. Custido, and J.P. Lobo Ferreria, Editor. 1988, D. Reidel: Norwell, Mass. p. 227-246.
38. LaBolle, E.M., G.E. Fogg, and A.F.B. Tompson, *Random-walk simulation of transport in heterogeneous porous media: Local mass-conservation problem and implementation methods.* Water Resources Research, 1996. **32**(3): p. 583-593.
39. Tompson, A.F.B. and L.W. Gelhar, *Numerical-Simulation of Solute Transport in 3-Dimensional, Randomly Heterogeneous Porous-Media.* Water Resources Research, 1990. **26**(10): p. 2541-2562.
40. Valocchi, A.J., and H. A. M. Quinodoz, *Application of the randomwalk method to simulate the transport of kinetically adsorbing solutes.* in Third IAHS Scientific Assembly, IAHS Publ., 1989. **185**: p. 35-42.
41. Michalak, A.M. and P.K. Kitanidis, *Macroscopic behavior and random-walk particle tracking of kinetically sorbing solutes.* Water Resources Research, 2000. **36**(8): p. 2133-2146.
42. Liu, H.H., G.S. Bodvarsson, and L. Pan, *Determination of particle transfer in random walk particle methods for fractured porous media.* Water Resources Research, 2000. **36**(3): p. 707-713.
43. Tompson, A.F.B. and D.E. Dougherty, *Particle-Grid Methods for Reacting Flows in Porous-Media with Application to Fisher Equation.* Applied Mathematical Modelling, 1992. **16**(7): p. 374-383.
44. Tompson, A.F.B., R. Ababou, and L.W. Gelhar, *Implementation of the 3-Dimensional Turning Bands Random Field Generator.* Water Resources Research, 1989. **25**(10): p. 2227-2243.
45. Ashby, S.F. and R.D. Falgout, *A parallel multigrid preconditioned conjugate gradient algorithm for groundwater flow simulations.* Nuclear Science and Engineering, 1996. **124**(1): p. 145-159.

46. Jones, J.E. and C.S. Woodward, *Newton-Krylov-multigrid solvers for large-scale, highly heterogeneous, variably saturated flow problems.* Advances in Water Resources, 2001. **24**(7): p. 763-774.
47. Kollet, S.J. and R.M. Maxwell, *Integrated surface-groundwater flow modeling: A free-surface overland flow boundary condition in a parallel groundwater flow model.* Advances in Water Resources, 2006. **29**(7): p. 945-958.
48. Doherty, J., *PEST: Model-independent parameter estimation, user manual, version 5*. 2004, Watermark Numer. Comput.: Brisbane, Aust.
49. Mutsvangwa, C., et al., *Application of Harvey-Garabedian model for describing bacterial removal in Sand Abstraction Systems associated with ephemeral rivers.* J Contam Hydrol, 2006. **88**(1-2): p. 55-68.
50. Anderson, M.P., *Characterization of geological heterogeneity*, in *Subsurface Flow and Transport: A Stochastic Approach*, G.D.a.S.P. Neuman, Editor. 1997, Cambridge University Press: UNESCO.
51. Zhu, J.F. and T.C.J. Yeh, *Characterization of aquifer heterogeneity using transient hydraulic tomography.* Water Resources Research, 2005. **41**(7): p. -.
52. Naff, R.L., in *A continuum approach to the study and determination of field longitudinal dispersion coefficients*. 1978, N. M. Inst. of Min. and Technol.: Socorro.
53. Morin, R.H., *Negative correlation between porosity and hydraulic conductivity in sand-and-gravel aquifers at Cape Cod, Massachusetts, USA.* Journal of Hydrology, 2006. **316**(1-4): p. 43-52.
54. Tompson, A.F.B. and K.J. Jackson, *Reactive transport in heterogeneous systems: An overview.* Reactive Transport in Porous Media, 1996. **34**: p. 269-310.

Acknowledgements

This material is based upon work supported by National Science Foundation **Grant # BES-0226460** and partly by the US Environmental Protection Agency under grants R-82818201-0 and CR83105801. Although the research described in this paper has been funded in part by the US Environmental Protection Agency, it has not been subjected to the Agency's required peer and policy review and therefore does not necessarily reflect the views of the Agency and no official endorsement should be inferred. Portions of this work were conducted under the auspices of the U. S. Department of Energy by the University of California, Lawrence Livermore National Laboratory (LLNL) under contract W-7405-Eng-48. The installation of well site F347 used in the 1987 bacterial transport test and test data relating to bacterial size distributions and concentration histories were collected with financial assistance from the USGS Toxic Substances Hydrology Program.

Table 1. Input Data for Particle Simulations

Parameter	Value	Reference
ρ_b	1720 kg/m^3	Harvey and Garabedian 1991
ρ	999 kg/m^3	Harvey and Garabedian 1991
ρ_p	1010 kg/m^3	Harvey et al., 1997
n	0.39	LeBlanc et al. 1991
H	3 x 10^{-21} kg m^2/s^2	Tufenkji and Elimelech, 2004
B_z	1.38 x 10 $^{-23}$ kg-m^2/s^{2}K	
T	288˚K	Harvey and Garabedian 1991
μ	1.14 x 10^{-3} kg/m-sec	Harvey and Garabedian 1991
d_p (average)	6.0 x 10^{-7} m	Harvey and Garabedian 1991
J (hydraulic gradient)	0.0015	LeBlanc et al. 1991
$\overline{K}$ at 9.1 m BLS[1]	78 m/d	Calculated from reported v, n, assumed J
$\overline{K}$ (fast zone) at 8.5 m BLS[1]	77 m/d	Calculated from reported v, n, assumed J
$\overline{K}$ (slow zone) at 8.5 m BLS[1]	58 m/d	Calculated from reported v, n, assumed J
α_L, α_T	0.0 m	Taken as zero in simulations, since effect of finite value was not discernable via test runs.
a_3	3.4 x 10^{-10}	From exponential fit to local-scale α_c –lnK data (Figure 4)
b_3	2.1	From exponential fit to local-scale α_c –lnK data (Figure 4)
δ_3	0	
a_2	9.46 10 $^{-7}$ sec $^{-1}$	From linear regression of detachment data in Schijven et al 1999
b_2	1.03 10^{-7} sec^{-1}	From linear regression of detachment data in Schijven et al 1999
δ_2	0	
σ_{lnK}^2	0.24	Hess et al., 1992
$\lambda_{x,y}$	3.5 m	Hess et al., 1992
λ_z	0.20 m	Hess et al., 1992

[1] used to assign initial values in parameter estimation procedure.

Table 2. Input and Final Calibration Parameters for Flow and Particle Models

Parameter	**Value**	**Unit**
dx	0.34	m
dy	0.34	m
dz	0.038	m
nx	50	
ny	30	
nz	100	
K_g_upper[1]	83	m/d
σ_{lnk}^2 _upper[1]	0.31	
K_g_lower[1]	87.5	m/d
σ_{lnk}^2 _lower[1]	0.22	
$\lambda_{x,y}$	3.60	m
λ_z	0.19	m
upper/lower domain split	8.91	m bls
domain size (x,y,z)	17.0 x 10.2 x 3.8	m
bottom of domain	10.41	m bls
Upper zone thickness	2.3	m
Lower zone thickness	1.5	m
Number of initial particles	75,000	
Maximum number of particles allowed after splitting	250,000	

[1]Final calibration values.

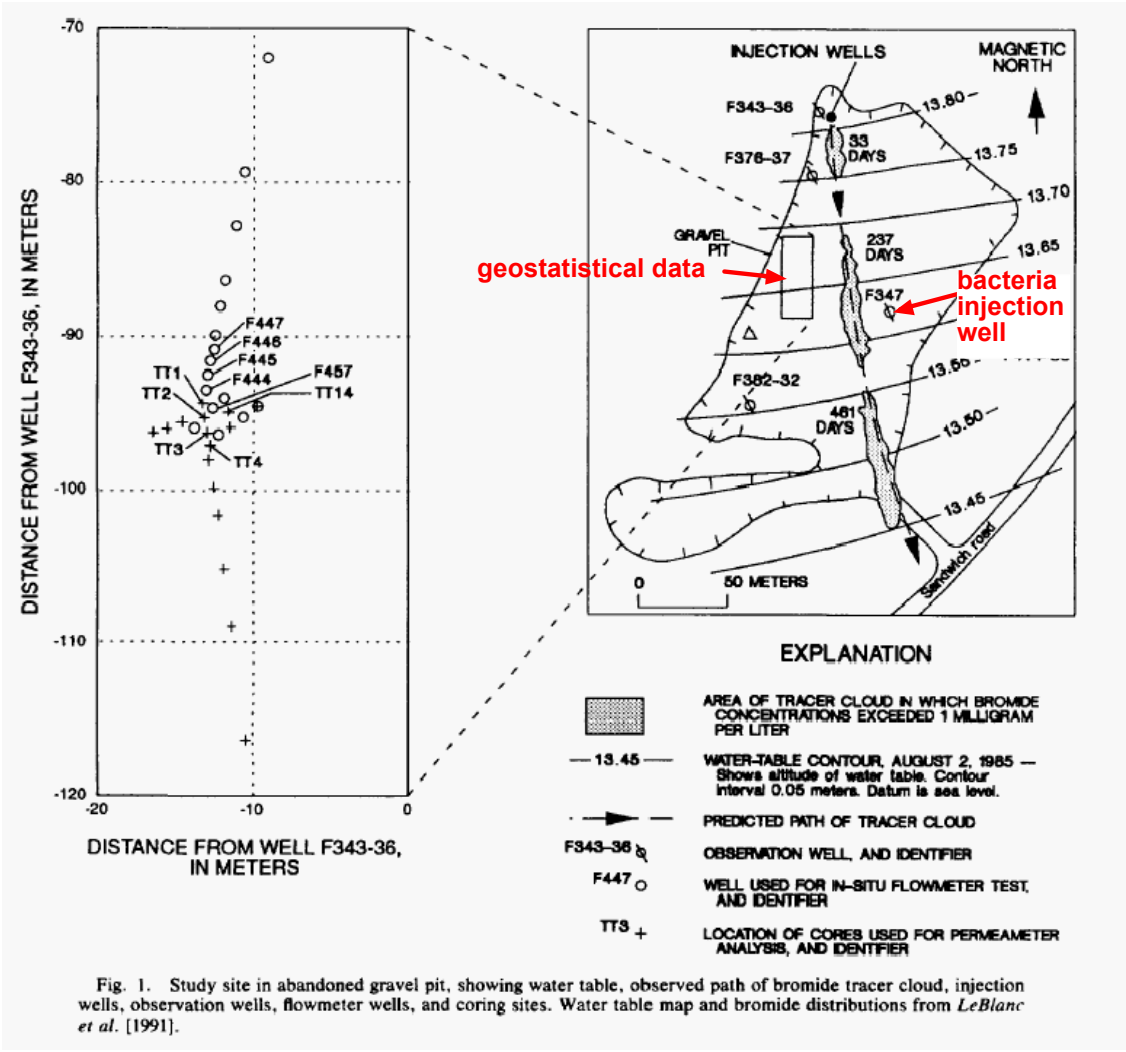

Fig. 1. Study site in abandoned gravel pit, showing water table, observed path of bromide tracer cloud, injection wells, observation wells, flowmeter wells, and coring sites. Water table map and bromide distributions from *LeBlanc et al.* [1991].

Figure 1. Location of the 1987 bacteria injection test [Harvey and Garabedian, 1991] in relation to the sample plot where characterization of the geostatistical distribution of aquifer properties [Hess et al., 1992] was carried out and to the trajectory of the bromide cloud created during an earlier large-scale conservative tracer study [LeBlanc et al ., 1991].

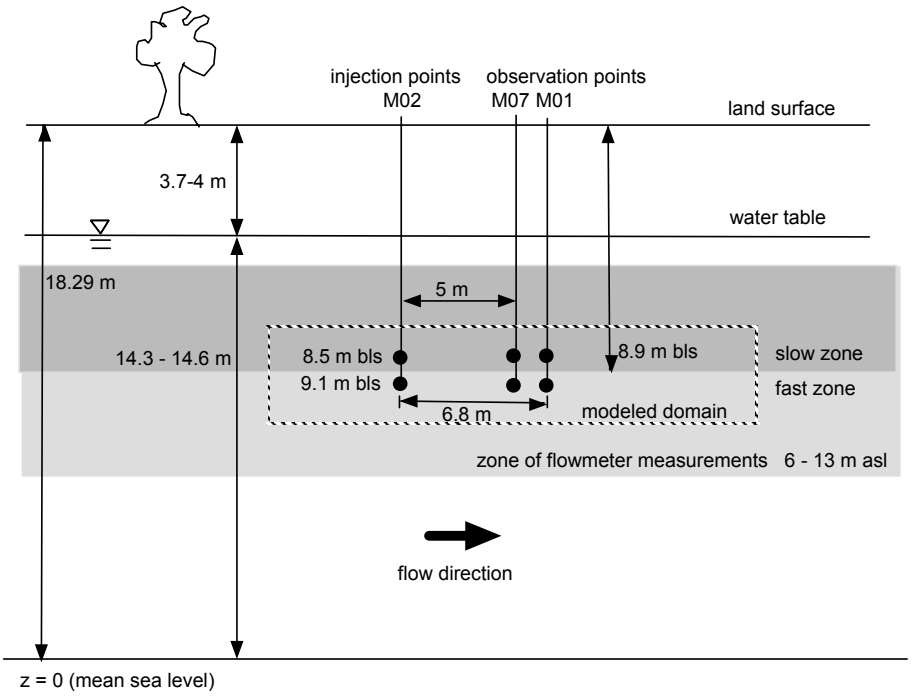

Figure 2. Location of injection and observation points for tracer test. Vertical extent of nearby Hess et al. [1992] flowmeter measurements used to calculate hydraulic conductivity is shown in gray. Fast and slow zones described by Harvey and Garabedian [1991] are depicted.

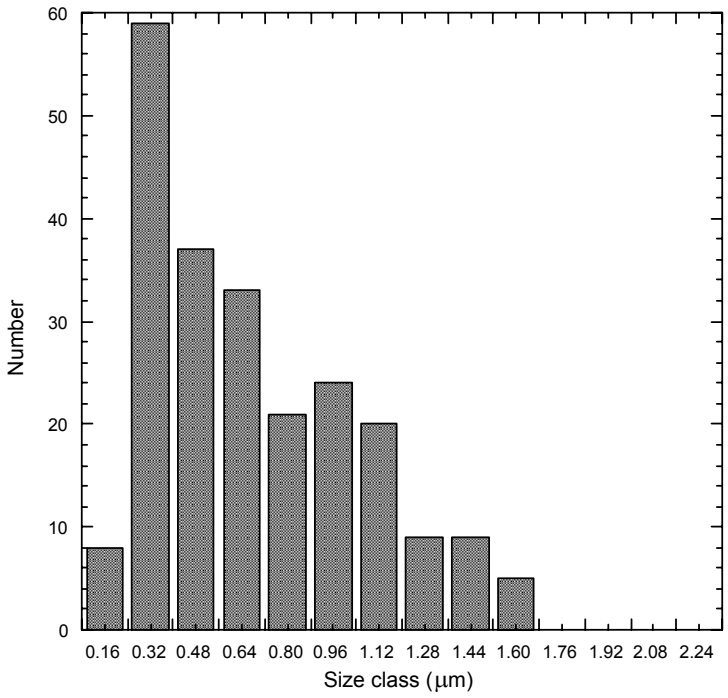

Figure 3. Distribution of diameters of indigenous bacteria injected in the 1987 tracer test [Field notes, R. W. Harvey].

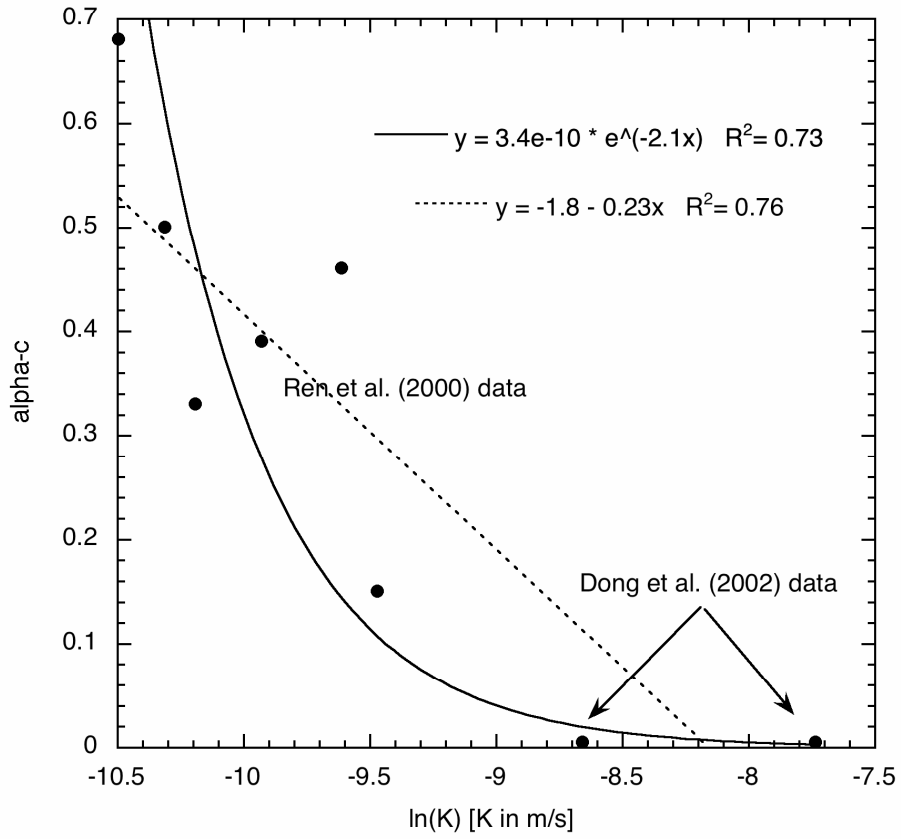

Figure 4. α_c vs. lnK data from Ren et al. (2000) and Dong et al. (2002) (as supplemented by Mailloux et al. 2003, Figure 10c) with linear and exponential fits to the data. The exponential fit was used in the model runs in this paper.

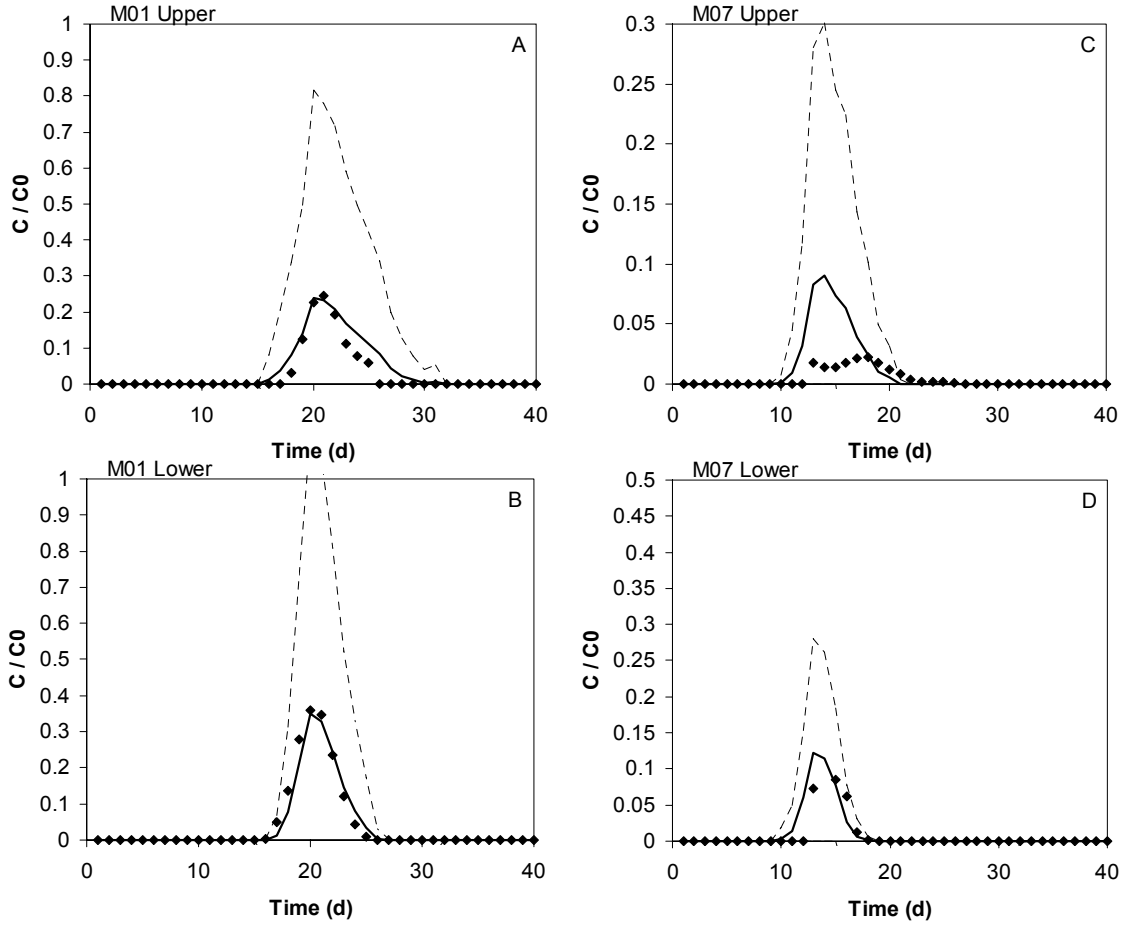

Figure 5. Plot of observed (symbols) and simulated (lines) bromide concentrations (normalized by initial concentration, C0) with time for both wells at both monitoring ports for the calibrated ensemble of realizations. Average simulated bromide plotted as a solid line with one standard deviation plotted as a dashed line.

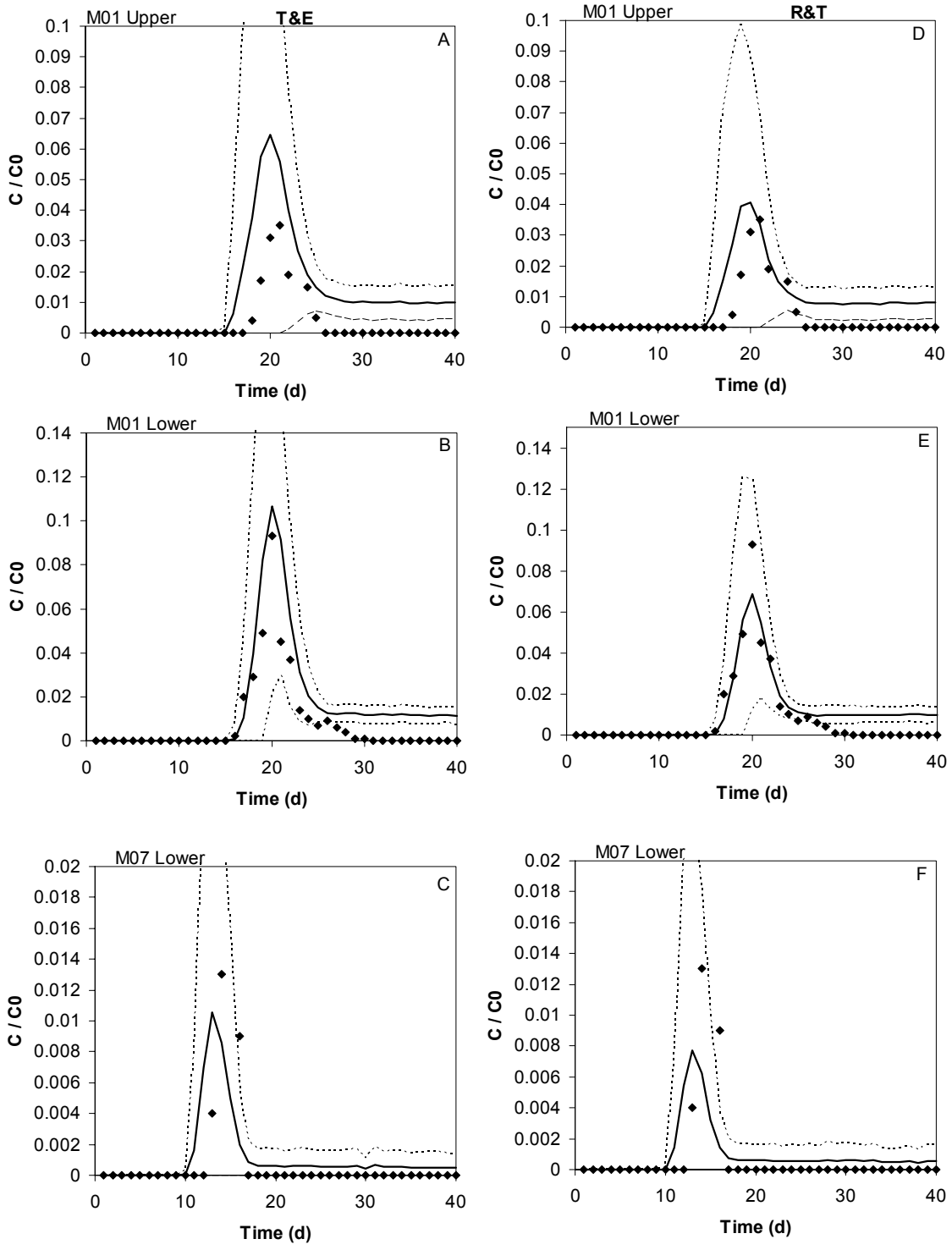

Figure 6. Plot of observed (symbols) and simulated (lines) bacterial concentrations (normalized by initial concentration, C0) with time for both wells for the T&E (left, A-C) and R&T (right, D-F) attachment formulation for an averaged particle size. Average simulated bacterial concentrations plotted as a solid line with plus/minus one standard deviation plotted as a dashed line.

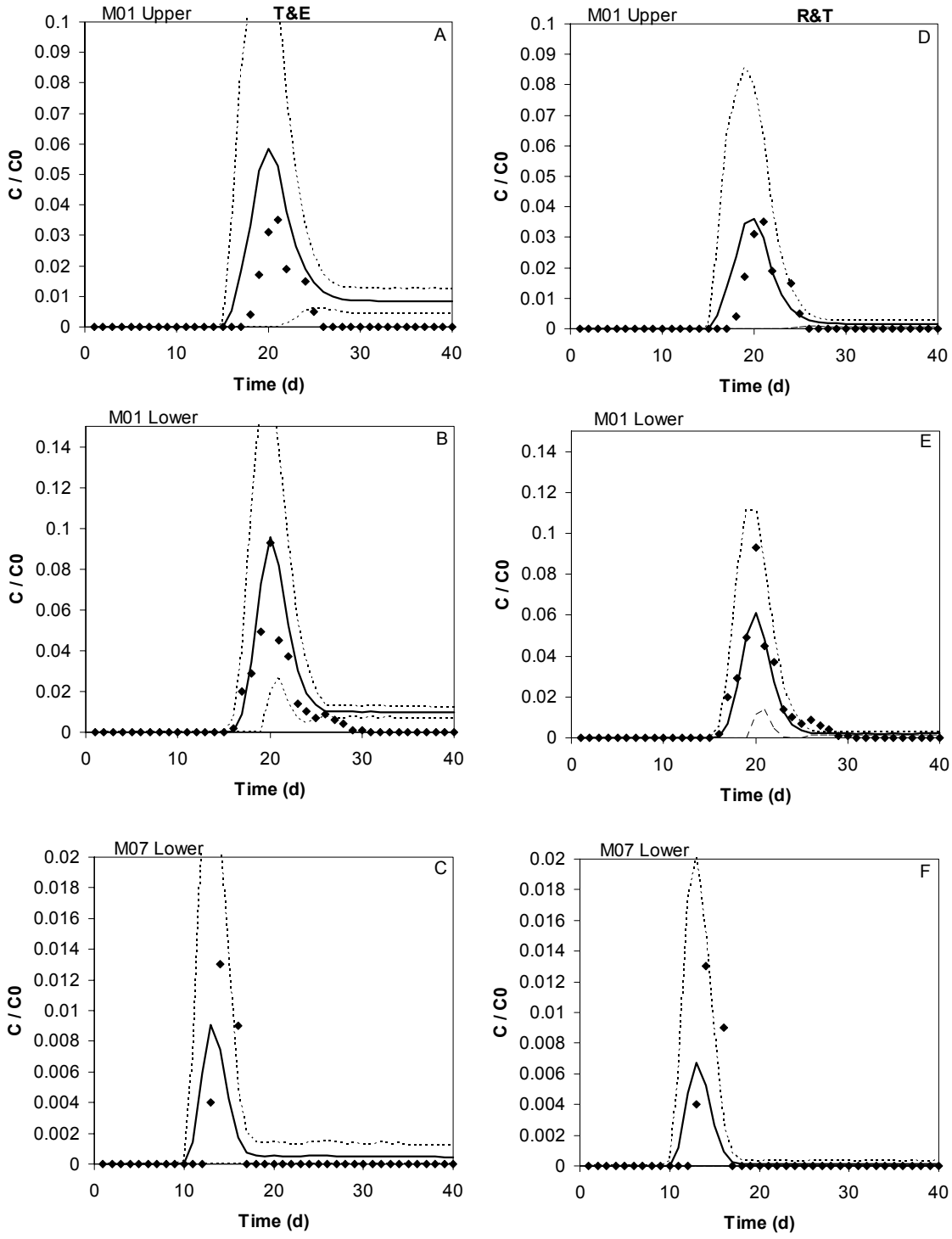

Figure 7. Plot of observed (symbols) and simulated (lines) bacterial concentrations (normalized by initial concentration, C0) with time for both wells for the T&E (left, A-C) and R&T (right, D-F) attachment formulation for the particle size distribution given in Figure 3. Average simulated bacterial concentrations plotted as a solid line with plus/minus one standard deviation plotted as a dashed line.

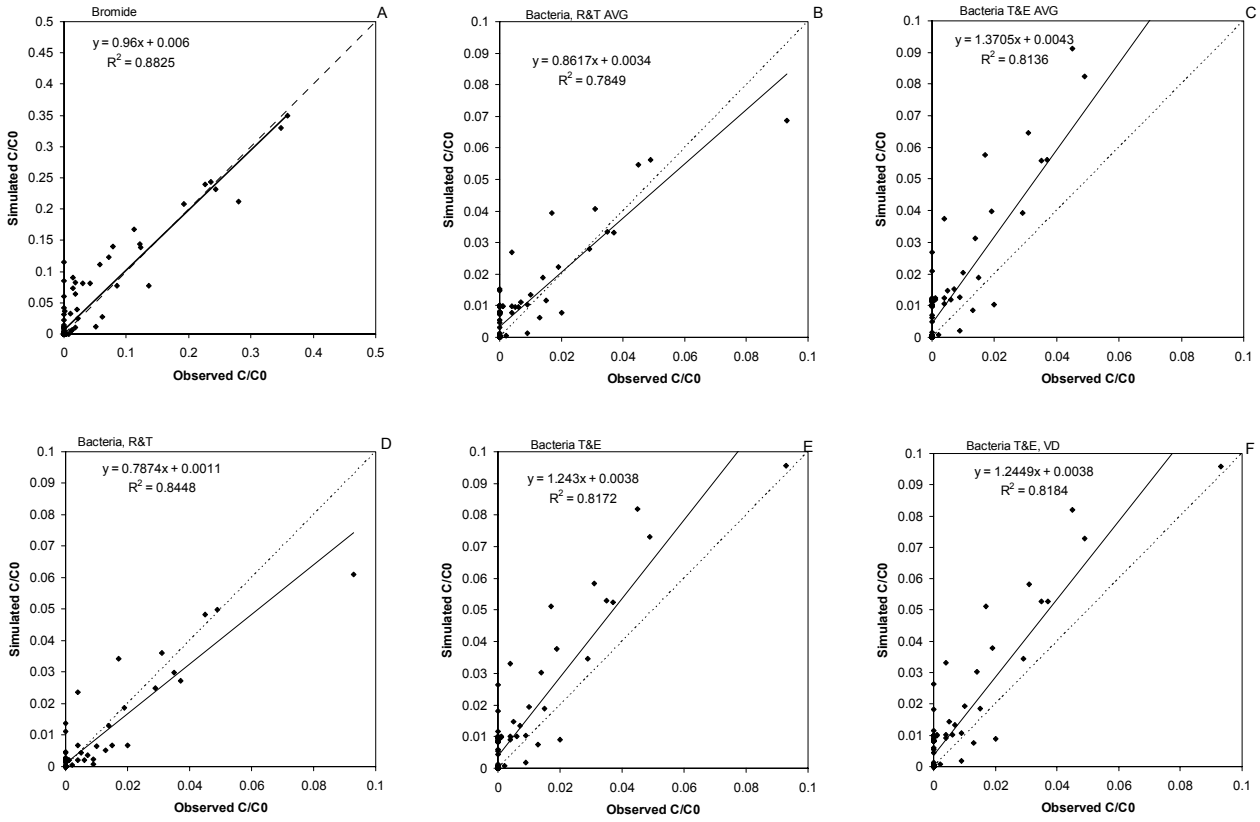

Figure 8. Plot of observed versus simulated averaged (arithmetic mean over all 100 realizations of hydraulic conductivity) concentrations for bromide and bacteria for all wells with 1 to 1 line (dotted) and linear fit noted on figure, for (a) bromide for all four monitoring locations; bacteria for the three non-zero monitoring locations for (b) constant diameter and R&T expression for η; (c) constant diameter with the T&E expression for η; (d) distribution of diameters and R&T expression for η; (e) distribution of diameters and T&E expression for η; and (f) distribution of diameters and R&T expression for η, with variable detachment.

Supplementary Information to "Revisiting the Cape Cod Bacteria Injection Experiment Using a Stochastic Modeling Approach"

Particle Transport Model Details

Particle-based numerical techniques have been widely utilized in solving equations for conservative and reactive chemical transport in porous media (e.g., Ahlstrom et al., 1977; Kinzelbach, 1988; Uffink, 1988, Tompson and Gelhar, 1990; Tompson and Dougherty, 1992; Tompson, 1993; Tompson, et al., 1996; Maxwell and Kastenberg, 1999; Abulaban and Nieber, 2000; Liu et al., 2000; Michalak and Kitanidis, 2000). Their performance is superior to many grid-based approaches at large grid-Peclet numbers in terms of numerical dispersion, spurious oscillations, and mass balance. The model utilized in this work and presented here is an adaptation of an algorithm developed by Lawrence Livermore National Lab for radionuclide transport (Maxwell and Tompson, 2006). The particle model is based on a version of the total mass balance equation in which physical and geochemical processes are simplified by assuming that the pH and groundwater composition are constant. The mass balance equations for the aqueous and attached phases are given by:

$$\frac{\partial C_j}{\partial t} + \nabla \bullet \left(\mathbf{v} C_j\right) - \nabla \bullet \left(\mathbf{D} \bullet \nabla C_j\right) = -k_j^{att} C_j + k_j^{\det} \frac{\rho_b}{\rho n} S_j \qquad (1a)$$

$$\frac{\rho_b}{\rho n} \frac{\partial S_j}{\partial t} = k_j^{att} C_j - k_j^{\det} \frac{\rho_b}{\rho n} S_j \qquad (1b)$$

where C_j represents the mass fraction of species j in solution, S_j is the mass fraction of attached species *j*, **v** is the average seepage velocity (L/t), *n* is the effective porosity,

k_j^{att} is the attachment rate of species j, $k_j^{\det}$ is the detachment rate of species j, and **D** is the hydrodynamic dispersion tensor. The hydrodynamic dispersion tensor ***D*** is defined as

$$\mathbf{D}(\mathbf{x}) = (\alpha_T V + D_e)\mathbf{I} + (\alpha_L - \alpha_T)\frac{\mathbf{vv}}{V} \tag{2}$$

where α_L and α_T are the longitudinal and transverse medium dispersivities (L), V is the magnitude of the seepage velocity, D_e is an effective molecular diffusivity (L^2/t) for the porous medium, and **I** is the identity matrix.

The spatial distribution of aqueous and attached microbial mass is approximated by a finite system of N_j particles

$$C_j(x,t) = \sum_{p=1}^{N_j^C} m_p^C \delta\left(x - X_p(t)\right) \tag{3a}$$

$$S_j(\mathrm{x},t) = \sum_{p=1}^{N_j^S} m_p^S \delta\left(\mathrm{x} - \mathrm{X}_p(t)\right) \tag{3b}$$

$$N_j = N_j^C + N_j^S \tag{3c}$$

where N_j^C is the number of particles in the aqueous phase, N_j^S is the number of attached particles, and δ is a Dirac function. The particles may be associated with different attributes such as mass (m_p^C, mass of particles in the aqueous phase; m_p^S, mass of attached particles), position ($\mathbf{X}_p$), type (j) (e.g., microbial species or attribute within a

species such as diameter), age ($t - t_0$) and phase of existence (e.g., free or attached) which is how particles are exchanged between C_j and S_j.

A simulation is initialized by mapping specified distributions of C_j, S_j and other relevant attributes onto a field of particles in a manner consistent with (3). The number of particles used to represent a unit of mass is defined as the particle resolution, N_r, and may be controlled to improve the quality of the solution. The simulation proceeds over discrete time steps by changing the various particle attributes. This involves moving the particles according to a known background velocity field and other medium characteristics associated with dispersion forces. The particle model is inherently mass conservative in the sense that the total mass between the free and attached states is conserved.

The movement of particles is based on an explicit random walk algorithm (Kinzelbach, 1988; Uffink, 1988, Tompson and Gelhar, 1990; Tompson, 1993; Maxwell and Kastenberg, 1999; Abulaban and Nieber, 2000),

$$\mathrm{X}_p(t+\Delta t) = \mathrm{X}_p(f) + \left(\mathbf{v} + \nabla \bullet \mathbf{D} + \mathbf{D} \bullet \nabla(\ln(n))\right)\Delta t + \mathbf{B} \bullet \mathbf{Z}\sqrt{\Delta t} \qquad (4)$$

In this expression, the second term on the right accounts for particle displacement along flow streamlines and includes two factors to correct for nonuniform distributions of n or $\mathbf{D}$. The porosity correction is usually a small quantity and is typically neglected. The third (random walk) term on the right accounts for the dispersive flux, where $\mathbf{B} \bullet \mathbf{B}^{\mathrm{T}} = 2\mathbf{D}$ and $\mathbf{Z}$ is a random vector whose independent components have zero mean and unit

variance. The particle mass density evolved through repeated use of (3) on all particles will satisfy a conservative (e.g., zero right-hand side) form of the simplified mass balance equation (1) in the limit as N_p or $N_r \to \infty$ (Tompson and Gelhar, 1990).

The time step, Δt, used in this algorithm is chosen uniquely for each individual particle as a function of accuracy limits imposed by the velocity field, in conjunction with other limits associated with the dispersion and attachment steps. This differs from the use of a uniform time step that may be used to advance the position of all particles simultaneously (e.g., as in Tompson and Gelhar, 1990). Typically, provisional values are chosen with respect to the constraints associated with each process, with the lowest value ultimately being selected for use. For example, the provisional time step associated with the displacement equation (4) is selected for each particle to advance it via advection along an interpolated streamline within each grid block, at most from one edge to the next (Pollock, 1988; Schafer-Perini and Wilson, 1991), but potentially over shorter distances if a change in the velocity field or constraints from other mechanisms dictate.

The advective substep is followed by other substeps that address the correction and random portions of the displacement shown in Equation 4. Provisional time steps are chosen independently for these steps as well, each limited by the magnitude of the velocity gradient or the largest dispersion coefficient. Because different time steps are used for different particles, periodic rendezvous times, *T*, may be identified to collect the position and state of all particles for visualization and other

interrogation purposes (Tompson et al., 1988; Maxwell, 1998; Maxwell and Kastenberg, 1999).

The effects of attachment and detachment (i.e. exchange of mass between Eq. 3a and 3b) is implemented into the particle model using a transitional probability approach, similar to that used by Liu et al. (2000) for approximating matrix diffusion and similar to Valocchi and Quinodoz (1989) for chemical sorption. During each time step, particles representing free bacteria, (3a) advected and dispersed using (4) may be transferred into stationary particles representing attached bacteria, (3b) and vice versa, as a probabilistic function of the time step. Particles that are attached to the soil matrix are not advected or diffused; their position remains fixed until they are probabilistically returned to the free regime.

For species *j*, the probability of a free bacteria attaching to the soil matrix is given by

$$P_{j,fa} = k_j^{att} \Delta t \tag{5}$$

and the probability of an attached bacteria moving back into solution is given by

$$P_{j,af} = k_j^{\det} \Delta t \tag{6}$$

Comparison of this method with the streamline approach used in Maxwell, et al. (2003) determined that the provisional time step associated with these transitional terms should be chosen such that $P_{j,fa}$ and $P_{j,af}$ are less than 0.02.

References

Abulaban, A., and J. L. Nieber (2000), Modeling the Effects of Nonlinear Equilibrium Sorption on the Transport of Solute Plumes in Saturated Heterogeneous Porous Media, *Advances in Water Resources* **23**(8), 893–905.

Ahlstrom, S., H. Foote, R. Arnett, C. Cole, and R. Serne (1977), *Multicomponent Mass Transport Model: Theory and numerical implementation*, Battelle Pacific Northwest Laboratories, Richland, WA, BNWL 2127.

Kinzelbach W, 1988. The random walk method in pollutant transport simulation, in Groundwater Flow and Quality Modeling, NATO ASI Ser., Ser. C Math and Phys. Sci., vol. 224, edited by E. Custido, A. Gurgui, and J.P. Lobo Ferreria, pp. 227-246, D. Reidel, Norwell, Mass.

LaBolle EM, Fogg GE, Tompson AFB, 1996. Random-walk simulation of transport in heterogeneous porous media: Local mass-conservation problem and implementation methods. Water Resour. Res., 32(3), 583-593

Liu, H. H., G. S. Bovarsson, and L. Pan (2000), Determination of Particle Transfer in Random Walk Particle Methods for Fractured Porous Media, *Water Resources Research* **36**(3), 707–713.

Maxwell, R.M. and W.E. Kastenberg, 1999. Stochastic environmental risk analysis: an integrated methodology for predicting cancer risk from contaminated groundwater. *Stochastic Environmental Research and Risk Assessment*, 13(1), 27-47, 1999.

Maxwell, R.M. and Tompson, A.F.B., 2006. SLIM-FAST User's Manual, Lawrence Livermore National Laboratory, Report UCID-xxxx, Livermore, CA, USA.

Michalak, A.M. and P.K. Kitanidis, 2000. Macroscopic behavior and random-walk particle

tracking of kinetically sorbing solutes, *Water Resources Research,* 36(8), 2133-2146.

Pollock, D. W. (1988), Semianalytical Computation of Path Lines for Finite-Difference Models, *Groundwater* **26**(6), 743–750.

Schafer-Perini AL, Wilson JL, 1991. Efficient and accurate front tracking for two-dimensional groundwater Fow models. Water Resour. Res., 27(7), 1471-1485.

Tompson, A. F. B., E. Vomvoris, and L. W. Gelhar (1988), *Numerical Simulation of Solute Transport in Randomly Heterogeneous Porous Media: Motivation, model development, and application, Technical Report 316*, Ralph M. Parsons Laboratory, Department of Civil Engineering, Massachusetts Institiute of Technology, Cambridge, 114 pp. (also Lawrence Livermore National Laboratory, Livermore, CA, UCID 21287, 1987).

Tompson AFB, Gelhar LW, 1990. Numerical simulation of solute transport in three-dimensional randomly heterogeneous porous media Water Resour. Res., 26(10), 2541-2562.

Tompson AFB, 1993. Numerical simulation of chemical migration in physically and chemically heterogeneous porous media. Water Resour. Res., 29(11), 3709-3726.

Tompson, A.F.B and D.E. Dougherty, 1992. Particle-grid methods for reacting flows in porous media with application to Fisher's equation. Appl. Math Modell., 16, 374-383.

Uffink GJM, 1988. Modeling of solute transport with random walk method, in Groundwater Flow and Quality Modeling, NATO ASI Ser., Ser. C Math and Phys. Sci., vol. 224, edited by E. Custido, A. Gurgui, and J.P. Lobo Ferreria, pp. 247-265, D. Reidel, Norwell, Mass.

Valocchi, A. J., and H. A. M. Quinodoz, 1989. Application of the randomwalk method to

simulate the transport of kinetically adsorbing solutes, in *Third IAHS Scientific Assembly*, IAHS Publ., 185, 35–42.